Fractals, Vol. 5, No. 1 (1997) 153–168

Conditional and Relative Multifractal Spectra

Rudolf H. Riedi
Mathematics Department, Yale University,
New Haven CT 06520-8283, USA – email: riedi@math.yale.edu
and
Projet Fractales, INRIA Rocquencourt,
B.P. 105, 78153 Le Chesnay Cedex, France – email: Rolf.Riedi@inria.fr
and
Istvan Scheuring
Institute for Advanced Study, Szentháromság utca 2
1014 Budapest, Hungary – email: schi@zeus.colbud.hu
Received May 28, 1996; Accepted Sept 27, 1996

Abstract

In the study of the involved geometry of singular distributions the use of fractal and multifractal analysis has shown results of outstanding significance. So far, the investigation has focussed on structures produced by one single mechanism which were analyzed with respect to the ordinary metric or volume. Most prominent examples include self-similar measures and attractors of dynamical systems. In certain cases, the multifractal spectrum is known explicitly, providing a characterization in terms of the geometrical properties of the singularities of a distribution. Unfortunately, strikingly different measures may possess identical spectra. To overcome this drawback we propose two novel methods, the *conditional* and the *relative* multifractal spectrum, which allow for a direct comparison of two distributions. These notions measure the extent to which the singularities of two distributions 'correlate'. Being based on multifractal concepts, however, they go beyond calculating correlations. As a particularly useful tool we develop the multifractal formalism and establish some basic properties of the new notions. With the simple example of Binomial multifractals we demonstrate how in the novel approach a distribution mimics a metric different from the usual one. Finally, the provided applications to real data show how to interpret the spectra in terms of mutual influence of dense and sparse parts of the distributions.

1 Introduction

Many nonlinear phenomena in physics, chemistry and biology are of a fractal and multifractal nature [23, 39, 18]. Prominent areas of application include, among many others, turbulence [23, 24, 6], and the study of protein surfaces [7]. In physics, it is natural to study the geometry and dynamics of one kind or category of objects. This situation, however, is rarely found in the most chemical, geological and biological systems. Many different components take part in chemical reactions, many different materials are dispersed in the soil, and a huge number of different plant and animal species live in a given habitat. As these components are not independent of each other, their interplay will be reflected by geometrical patterns of such systems. In vegetation science, e.g. a question of considerable importance is the association and dissociation of the different elements as well as the scale dependence of these relations.

In this paper we propose two extensions of multifractal analysis which apply to geometrical objects consisting of different categories of points. In a previous paper [37], the authors have described a first algorithm which provides a *conditional multifractal spectrum*. Here, this notion will be compared with a more sophisticated approach: the *relative multifractal spectrum*. This procedure generalizes the usual multifractal analysis in providing information on the geometrical manifestation of complex dynamical relations among the two distributions. Since our approach involves all the moments of the distributions, we go beyond computing correlations. With the relative spectrum we touch on ideas which come close to original works by Caratheodory [31] and Billingsley [3].

The structure of the paper is as follows: In Section 2 we introduce multifractal analysis and recall some simple properties. Section 3 is devoted to the novel notions which are discussed in a simple situation (Subsection 3.3) as well as in general (Subsection 3.4). In Section 4 we introduce numerical algorithms and compare them. In addition, we elaborate on the geometrical interpretation of the new notions. An Appendix gives further mathematical details.

2 Multifractal analysis: Preliminaries.

2.1 The Binomial Measure

Purpose and techniques of multifractal analysis are best explained in the most simple situation: the binomial measure.

This probability measure μ is constructed by splitting $I := [0,1]$ into two subintervals I_0 and I_1 of equal length and assigning the masses m_0 and $m_1 = 1 - m_0$ to them. With the two subintervals one proceeds in the same manner and so forth: at stage two, e.g. the four subintervals I_{00}, I_{01}, I_{10}, and I_{11} have masses $m_0 m_0$, $m_0 m_1$, $m_1 m_0$, and $m_1 m_1$ respectively. At stage n, the mass of μ is distributed among the 2^n intervals $I_{\varepsilon_1 \ldots \varepsilon_n}$ according to all possible products: $\mu(I_{\varepsilon_1 \ldots \varepsilon_n}) = m_{\varepsilon_1} \cdot \ldots \cdot m_{\varepsilon_n}$. By construction, the restrictions of μ to the intervals I_0 and I_1 have the same structure as μ itself. Thus, μ is *self-similar* in a very strict way.

Another way of defining μ is the following. Let $x = .\sigma_1\sigma_2\ldots$ be the dyadic representation of a point in $[0,1]$. Here, we don't have to care about points with multiple expansions since our results concern 'almost all points x'. Imagine that the digits σ_k are picked randomly such that $P[\sigma_k = i] = m_i$ independently of k. Then, μ is the law—or probability distribution—of the corresponding x on $[0,1]$.

This distribution clearly has no density, unless $m_0 = m_1 = 1/2$. More precisely, $M(x) = \mu([0,x])$ has zero derivative almost everywhere. Nevertheless, any coarse graining of μ, e.g. through dyadic intervals $I_{\varepsilon_1 \ldots \varepsilon_n}$ as above, will naturally result in a distribution with density. It is, therefore, essential to understand the limit behavior of such an approximation.

Let $I^{(n)}(x)$ denote the unique dyadic interval of order n containing x. Set

$$\alpha_n(x) := \frac{\log \mu\big(I^{(n)}(x)\big)}{\log |I^{(n)}(x)|} = -\frac{1}{n} \log_2 \mu\big(I^{(n)}(x)\big).$$

For the binomial measure as introduced above, the Law of Large Numbers implies for (Lebesgue) almost all x:

$$\begin{aligned} \alpha_n(x) &= -\frac{1}{n}\sum_{k=1}^{n} \log_2 m_{\sigma_k} \to \mathbb{E}_\lambda[-\log_2 m_{\sigma_i}] \\ &= -\frac{1}{2}\log_2 m_0 m_1 > 1, \end{aligned}$$

hence, $M'(x) = 0$ indeed. For μ-almost all x, i.e. for almost all points x picked randomly according to the probability distribution μ, the LLN gives

$$\begin{aligned} \alpha_n(x) &\to \mathbb{E}_\mu[-\log_2 m_{\sigma_i}] \\ &= -m_0 \log_2(m_0) - m_1 \log_2(m_1). \end{aligned} \quad (1)$$

More precise information on limits $\alpha(x) = \lim_{n\to\infty} \alpha_n(x)$ is provided by so-called large deviation theorems [10]. Consider the sequence of random variables $Y_n = \log \mu\big(I_K^{(n)}\big)$ where the dyadic interval $I_K^{(n)}$ of order n has been chosen randomly with uniform distribution, i.e. $P_n[I_{K(\omega)}^{(n)} = I_k^{(n)}] = 1/2^n$ for all $k = 1, \ldots, 2^n$. In order to apply Ellis' theorem [10, Thm 2] one has to calculate the asymptotic behavior of its moment generating functions:

$$\begin{aligned}
\mathbb{E}_n[\exp(qY_n)] &= 2^{-n} \sum_{k=1}^{2^n} \mu\big(I_k^{(n)}\big)^q \\
&= 2^{-n}\left(m_0^q + m_1^q\right)^n .
\end{aligned}$$

Thus,

$$\begin{aligned}
c(q) &:= \lim_{n\to\infty} -\frac{1}{n} \log_2 \mathbb{E}_n[\exp(qY_n)] \\
&= 1 - \log_2\left(m_0^q + m_1^q\right).
\end{aligned}$$

Since c is a differentiable, concave function, we conclude with Ellis' theorem on Large Deviations that

$$\frac{1}{n}\log_2 P_n\Big[\frac{-1}{n\log 2} Y_n \in (\alpha - \varepsilon, \alpha + \varepsilon)\Big] \quad \to \quad c^*(\alpha) \qquad (n \to \infty, \varepsilon \to 0). \tag{2}$$

Here, c^* denotes the Legendre transform as usual, i.e.

$$c^*(\alpha) = \inf_q (q\alpha - c(q)). \tag{3}$$

Noting that the distribution P_n essentially reduces to counting, and that

$$\frac{-1}{n\log 2} Y_n = \frac{\log \mu\big(I_K^{(n)}\big)}{\log |I_K^{(n)}|} =: \alpha\big(I_K^{(n)}\big)$$

is in fact the *coarse Hölder exponent* of the dyadic intervals of order n we may interpret this results in terms of a *coarse graining* approach to a description of the multiplicative structure of the measure μ.

It is worthwhile looking more carefully into the Large Deviation result. Its proof involves a 'change of probability' meaning that the intervals $I_k^{(n)}$ are chosen randomly according to a law μ_q which insures the almost sure convergence of $\alpha(I_k^{(n)})$ towards some value α_q. This distribution μ_q is defined in the same way as μ but with probabilities $\overline{m}_0 := m_0^q 2^\beta$ and $\overline{m}_1 := m_1^q 2^\beta$ with $\overline{m}_0 + \overline{m}_1 = 1$, i.e.

$$\beta(q) := -\log_2\left(m_0^q + m_1^q\right).$$

Choosing the digits σ_k of the dyadic expansion of a point x such that $P[\sigma_k = i] = m_i^q 2^\beta$ amounts to picking x randomly with law μ_q. Then, μ_q–almost surely

$$\begin{aligned}
\alpha_n(x) &\to \mathbb{E}_{\mu_q}[-\log_2(m_{\sigma_i})] \\
&= -\sum_{i=0}^{1} \overline{m}_i \log_2 m_i = \beta'(q)
\end{aligned}$$

by the LLN, whence the claimed almost sure convergence with $\alpha_q := \beta'(q)$.

Moreover, we find that

$$\begin{aligned}
\frac{\log \mu_q\big(I^{(n)}(x)\big)}{\log |I^{(n)}(x)|} &= \frac{-1}{n}\log_2 \mu_q\big(I^{(n)}(x)\big) \\
&\to q\alpha_q - \beta(q) = \beta^*(\alpha_q)
\end{aligned}$$

μ_q almost surely. In other words, μ_q is essentially equivalent to the $\beta^*(\alpha_q)$-dimensional Hausdorff measure [11] on the 'set of Hölder exponent α_q'. Thus, $\beta^*(\alpha_q)$ *is* the dimension [11] of this set.

In summary, we verified that in this simple situation three approaches are closely linked: one through a 'partition function', one through 'counting' and one using the concept of 'dimensions'. In a notion which we are about to introduce this reads as

$$\beta^*(\alpha) = f_{\mathrm{G}}(\alpha) = f_{\mathrm{h}}(\alpha).$$

This relation, sometimes called the multifractal formalism, has been the object of intense study [1, 9, 33].

2.2 The multifractal spectra

A distribution of points in d-space is usually given in form of a measure μ: the probability for a point to fall in a set E is $\mu(E)$. If this distribution is singular one cannot describe it by means of a density and multifractal analysis proves useful in characterizing the complicated geometrical properties of μ. The basic idea is to classify the singularities of μ by strength. This strength is measured as a singularity exponent $\alpha(x)$. Usually, points of equal strength lie on interwoven fractal sets K_α:

$$K_\alpha := \Big\{x \in \mathbb{R}^d \,:\, \alpha(x) := \lim_{B\to\{x\}} \frac{\log \mu(B)}{\log |B|} = \alpha\Big\}.$$

Here, $B \to \{x\}$ means that B is a ball containing x, and that its diameter $|B|$ tends to zero. The geometry of the singular distribution μ can then be characterized by giving the 'size' of the sets K_α, more precisely, their Hausdorff dimension [11]:

$$f_{\mathrm{h}}(\alpha) := \dim(K_\alpha).$$

In applications, however, one considers a *coarse grained* version $f_{\rm G}$ which was in fact introduced prior to $f_{\rm h}$ [23, 24, 13, 12, 19, 17, 20]:

$$f_{\rm G}(\alpha) := \lim_{\varepsilon\to 0}\limsup_{\delta\to 0}\frac{\log N_\delta(\alpha,\varepsilon)}{\log 1/\delta}$$

Here N_δ denotes the number of 'cubes of size δ with coarse Hölder exponent $\alpha(C)$ roughly equal to α'. More precisely, let G_δ be the set of all cubes $C = [l_1\delta,(l_1+1)\delta)\times\ldots\times[l_d\delta,(l_d+1)\delta)$ in d-dimenional space with integer $l_1,\ldots,l_d$ and with $\mu(C)\neq 0$, i.e. C contains at least one point of the distribution. Let $C^* := [(l_1-1)\delta,(l_1+2)\delta)\times\ldots\times[(l_d-1)\delta,(l_d+2)\delta)$ denote the concentric cube of triple size and define

$$\alpha(C) := \frac{\log\mu(C^*)}{\log|C|}.$$

Then,

$$N_\delta(\alpha,\varepsilon) = \#\{C\in G_\delta\ :\ \alpha(C)\in(\alpha-\varepsilon,\alpha+\varepsilon]\}.$$

As was described earlier in [33, 28], the straightforward way of defining $\alpha(C)$ by $\log\mu(C)/\log|C|$ gives poor results in theory as well as in numerical application. In particular, it is inevitable to perform some averaging. Among the various possible improvements [21, 34, 38] we favor the given one for its simplicity and accuracy.

Though tempting it is *wrong* to interpret $f_{\rm G}$ as the box dimension of K_α. This function is better explained in statistical terms: Pick a cube C out of G_δ randomly and determine its *coarse Hölder exponent* $\alpha(C) := \log\mu(C^*)/\log\delta$. Then, the probability of finding $\alpha(C)\simeq\alpha$ behaves roughly like

$$N_\delta(\alpha,\varepsilon)/N_\delta = P_\delta[\alpha(C)\simeq\alpha]\simeq\delta^{D-f_G(\alpha)}. \qquad (4)$$

Here, N_δ denote the total number of δ-cubes which contain a point of the distribution μ. D denotes the box dimension of the support of μ, i.e. $N_\delta\simeq\delta^{-D}$. Hence, $f_{\rm G}(\alpha)\leq D$. We conclude with (4) that in the limit $\delta\to 0$ the only Hölder exponent which is observed with non-vanishing probability is α_0, where $f(\alpha_0)=D$.

For self-similar measures, the existence of α_0 can be viewed as a simple consequence of the Law of Large Numbers (LLN). Write

$$\begin{aligned}\alpha(x) &= \lim_{n\to\infty} -\frac{1}{n}\log_2\mu(C_n^*(x))\\ &= \lim_{n\to\infty} -\sum_{k=1}^{n}\frac{1}{n}\log_2\frac{\mu(C_n^*(x))}{\mu(C_{n-1}^*(x))}\end{aligned}$$

where $C_n(x)$ is the unique cube in $G_{1/2^n}$ containing x. The assumption of self-similarity implies that $\log_2\mu(C_n^*(x))/\mu(C_{n-1}^*(x))$ is of equal distribution for all n. (Compare Subsection 2.1 and [33].) Letting α_0 denote the common expected value, the LLN implies that almost surely $\alpha(x)=\alpha_0$ when picking points x randomly with 'uniform' distribution.

It is clear, on the other hand, that α_0 is in general not the only limiting Hölder exponent $\alpha(x)$ that can occur. More precisely, on every finite level of approximation one will have a whole histogram of *coarse Hölder exponents* $\alpha(I_k^{(n)})$. The probability of finding $\alpha(I_k^{(n)})\simeq\alpha\neq\alpha_0$, however, will decrease exponentially to 0. This is in essential the content of the theory of large deviations. The theorem of Ellis [10] (compare also (2)), e.g. implies that

$$P_n[-\frac{1}{n}\log_2\mu(C_n^*(x))\simeq\alpha]\simeq 2^{nc^*(\alpha)}$$

with $c^*(\alpha)<0$ unless $\alpha=\alpha_0$. The rate of convergence $c^*(\alpha)$ is obtained as the Legendre transform of the "moment generating function"

$$c(q) := \lim_{n\to\infty}\frac{-1}{n}\log_2\mathbb{E}[\exp\{q\log_2\mu(C_n^*(x))\}]$$

The better known *partition function* $\tau(q)$

$$\tau(q) = \lim_{\delta\to 0}\frac{\log\sum_{C\in G_\delta}\mu(C^*)^q}{\log\delta}$$

equals c up to a constant. Indeed, since $D=-\tau(0)$ by definition, we find

$$c(q)=\tau(q)-\tau(0).$$

Combining this with (2), (3) and (4) we obtain what is called the *multifractal formalism* (provided Ellis' theorem applies):

$$f_{\rm G}(\alpha)=\tau^*(\alpha).$$

The similarity to the well-known thermodynamical formalism [39, 34] is immediate.

2.3 The multifractal formalism

One of the powers of Ellis' theorem on Large Deviations is that it holds for very general sequences of random variables Y_n, as compared to the LLN. It assumes, however, that $\tau(q)$ is differentiable. If so, we find that $f_{\rm G}$ is the Legendre transform of $\tau(q)$ as above, and the *multifractal formalism* holds. In general, however, $\tau(q)$ is not differentiable everywhere, as examples prove. The opposite relation, on the other hand,

$$\tau(q) = f_{\mathrm{G}}^*(q) = \inf_{\alpha\in\mathbb{R}} \Big(q\alpha - f_{\mathrm{G}}(\alpha)\Big) \qquad (5)$$

holds always as has been shown in [33]. This answers a question raised in [9]. As a consequence, $f_{\mathrm{G}}(\alpha_0) = D = -\tau(0)$ and $\alpha_0 = \tau'(0)$. Though there are simple and convincing counterexamples [33, 35, 36], $f_{\mathrm{G}}(\alpha)$ is concave in a typical point and can be computed from $\tau(q)$. In particular, we have [34]:

$$\begin{array}{rclr} f_{\mathrm{G}}(\alpha^+) & = & q\alpha^+ - \tau(q) & (q>0) \\ f_{\mathrm{G}}(\alpha^-) & = & q\alpha^- - \tau(q) & (q<0) \end{array} \qquad (6)$$

where $\alpha^+ := \tau'(q+)$ and $\alpha^- := \tau'(q-)$ denote the one-sided derivatives of $\tau(q)$.

Since $\tau(q)$ is obtained by averaging, it depends more regularly on the data than $f_{\mathrm{G}}(\alpha)$ and is easier to compute. Therefore, the so-called *generalized dimensions*

$$D(q) := \frac{\tau(q)}{q-1}$$

have been of major interest in numerical approaches to multifractal analysis. Besides $D = D_0$, a notable Hölder exponent is $\alpha_1 = \tau'(1) = D_1$. It has been termed information dimension [14, 15, 16, 27]: With respect to the given distribution μ we have $\alpha(x) = \alpha_1 = D_1$ almost surely. For a binomial measure α_1 is given by (1).

Finally, we are in the position to explain our choosing the enlarged and concentric cubes C^* in our numerical approach. First of all, the enlarged cubes C^* provide a better approximation of a ball centered in a point of the distribution than the cube C itself. A cube C which contains only one or a few points close to its boundary has a mass $\mu(C)$ which is unnaturally small with respect to its size δ. For negative q, these undesired terms will influence the asymptotic behavior of the partition sum, and thus, the numerical estimate of $\tau(q)$ and $D(q)$. In particular, for a partition sum which uses C instead of C^* the multifractal formalism breaks down for $q < 0$. Indeed, as is explained in more detail in [33, 28], this is the major source for numerical instability.

3 Multifractal analysis with arbitrary reference measure

It would be possible to introduce our new notions mentioning only $D(q)$. In particular, we will extend the multifractal notions only for the coarse graining approach, especially since f_{h} does not generalize so easily. We feel, however, that including f_{G} provides a deeper understanding.

3.1 Conditional multifractal spectrum

Assume now that a second distribution π is given which we will address as *reference distribution.* Instead of performing a multifractal analysis of μ as described above one would like to study how the singular behavior of μ and π correlate, if at all. Such a knowledge could, e.g. provide information on how two growing systems depend on one another.

In a first attempt, [37] introduced the *conditional partition function* which differs only slightly from $\tau(q)$:

$$\tau_C(q) := \liminf_{\delta\to 0} \frac{\log \sum_{\pi(C)\neq 0} \left(\mu(C^*)/T_\delta\right)^q}{\log \delta}.$$

This definition means that we consider only cubes C which contain at least one point of the reference distribution π. Note, that we normalize by dividing μ by the total mass of these cubes $T_\delta := \sum_{\pi(C)\neq 0} \mu(C^*)$.

This procedure is simple and, yet, has been shown to yield significant information [37]. As one particular result we mention that $\tau_C(q)$ is the Legendre transform of a properly defined spectrum, i.e. a relation analogous to (5) holds. Consequently, $\tau_C(q)$ is convex and the *conditional multifractal dimensions*

$$D_C(q) := \frac{\tau_C(q)}{q-1}$$

are monotonous as a function of q. As is demonstrated in [2] there is a method for proving the monotony of $D(q)$ without using the Legendre transform. The same argument applies also to $D_C(q)$, as is easely seen, but not to $D_R(q)$ (see corollary 1).

Unfortunately, this notion reflects the geometry of π only in a very crude way, and it is not sensibly to the fine details. Therefore, it is desirable to introduce a second notion which is closer related to f_{G}.

3.2 Relative multifractal spectrum

The second and more involved notion bound to quantify the influence of two distributions on the geometry of each other touches on an idea as simple as the first one. The idea is to replace the diameter – or $1/d$-th power of the volume – $|B|$ in the usual definition of Hölder exponents by a general measure. More precisely, given an arbitrary *reference distribution* π we study the *relative Hölder exponents*

$$\alpha^{\mu/\pi}(x) := \lim_{B\to\{x\}} \frac{\log\mu(B)}{\log\pi(B)}.$$

The two measures μ and π have equal rights, since $\alpha^{\mu/\pi} = 1/\alpha^{\pi/\mu}$.

Persuing the idea of replacing $|\cdot|$ by π consequently, the coarse grained version uses a partition of space into sets of equal π-measure instead of equal size. Though this procedure is clear as long as we work on the line and as long as the reference measure π is non-atomic, more care is needed in the general case. Therefore, let us begin by mentioning that the usual scaling law $\sum\mu(C^*)^q \simeq \delta^\tau$ can be rewritten as $\sum\mu(C^*)^q|C^*|^{-\tau} \simeq$ constant. In this form, the generalization is straightforward. Consider the 'partition sum'

$$S_\delta(q,t) := \sum_{\mu(C)\neq 0\neq\pi(C),\, C\in H_\delta} \mu(C^*)^q\pi(C^*)^{-t}$$

and define the *relative partition function* $\tau_R(q)$ and the *relative multifractal dimensions* $D_R(q)$ through

$$\begin{aligned} \tau_R(q) &:= \sup\{t\in\mathbb{R} : S_\delta(q,t)\to 0 \text{ as } (\delta\to 0)\} \\ D_R(q) &:= \frac{\tau_R(q)}{q-1}. \end{aligned}$$

Notice that we did not specify the partition H_δ. As the general approach of Caratheodory [31] shows, this does not matter as long as a reasonable notion of 'size' $\Psi(C)$ goes to zero for all $C\in H_\delta$ as $\delta\to 0$. Moreover, $\tau_R(q)$ can be fairly called a dimension.

With regard to our substituting $|\cdot|$ by π as the reference measure we divide each cube C repeatedly into 2^d subcubes until the π-measure drops the first time below δ. This leads to a partition H_δ of space into cubes of π-mass approximately equal to δ. Certainly, $\Psi(C)=\pi(C)$ is a 'reasonable notion of size'. It is clear that the usual partition G_δ is recovered if π happens to be 'volume', or equivalently $|\cdot|$. The choice of the partition H_δ has advantages in the numerical estimation of $\tau_R(q)$ as is elaborated in Section 4.

The coarse grained *relative multifractal spectrum* $f_R(\alpha)$ is defined in a similar way as $f_{\mathrm{G}}(\alpha)$:

$$f_R(\alpha) := \lim_{\varepsilon\to 0}\limsup_{\delta\to 0}\frac{\log M_\delta(\alpha,\varepsilon)}{\log 1/\delta}$$

with

$$\begin{aligned} M_\delta(\alpha,\varepsilon) &= \#\{C\in H_\delta : \\ &\qquad \pi(C^*)^{\alpha+\varepsilon}\le\mu(C^*)<\pi(C^*)^{\alpha-\varepsilon}\}. \end{aligned}$$

We postpone a general, but more sophisticated definition to the Appendix A. There, we also demonstrate that $\tau_R(q)$ and $f_R(\alpha)$ are related in the same fashion as $\tau(q)$ and $f_{\mathrm{G}}(\alpha)$ (see (5)):

Lemma 1

$$\tau_R(q) = f_R{}^*(q) = \inf_{\alpha\in\mathbb{R}}\Big(q\alpha - f_R(\alpha)\Big).$$

As special cases we mention

- $(\pi=\mu)$: The relative spectrum f_R of a measure with respect to itself is trivial and consists only of the point $(1,D)$. The conditional spectrum, on the other hand, coincides with the usual multifractal spectrum: $f_{\mathrm{C}} = f_{\mathrm{G}}$.
- $(\pi = |\cdot|)$: If the reference measure happens to be 'volume$^{1/d}$' we fall back onto the classical definition: $f_{\mathrm{G}} = f_{\mathrm{C}} = f_R$.
- $(\mu = |\cdot|)$: To compute the relative or conditional spectrum of Lebesgue measure with respect to a measure π can be interpretated in two ways. First, it means to compute the 'fixed mass spectrum' [34] of this measure π, provided π is continuous and non-vanishing. Secondly, for measures on the line it amounts also to computing the spectrum of the 'inverse measure' of π [25, 35, 36].

At this point, it is due to refer to J. Lvy Vhel and R. Vojak [22] who independently developed a theory of a 'mutual multifractal analysis' based on similar ideas. Their interest lies in discovering Hölder exponents of a measure hidden by the exponents of another, superposed measure, as well as in proving that virtually any function can be observed as the spectrum f_{h} of so-called sequences of 'Choquet capacities'. As they point out in addition, changing the reference measure may improve the convergence of multifractal spectra. Functions similar to our $S_\delta(q,t)$ have also been used by Brown, Michon & Perière [4] and can be found in works as early as Caratheodory [31] and Billingsley [3], however, with a different object.

Next, we present an example where calculations can be carried out explicitly. This allows to demonstrate the main features of the approach in clear light. The general case will be discussed in Subsection 3.4 and Section 4.

3.3 The binomial measures revisited

Let us illustrate the new notions in the simple situation of two binomial measures μ and π. As described in Subsection 2.1 these measure are constructed by splitting $I := [0,1]$ into two subintervals I_0 and I_1 of equal length and assigning mass m_0, m_1, resp. p_0, p_1 to them ($m_0 + m_1 = 1$, $p_0 + p_1 = 1$). At stage n, the mass of μ, resp. π is distributed among the 2^n intervals $I_{\varepsilon_1 \ldots \varepsilon_n}$ according to all possible products: $\mu(I_{\varepsilon_1\ldots\varepsilon_n}) = m_{\varepsilon_1} \cdot \ldots \cdot m_{\varepsilon_n}$ and $\pi(I_{\varepsilon_1\ldots\varepsilon_n}) = p_{\varepsilon_1} \cdot \ldots \cdot p_{\varepsilon_n}$, respectively.

In order to determine the multifractal spectrum it is easiest to think of the points $x \in [0,1]$ as being representated by dyadic expansion $x = .\varepsilon_1\varepsilon_2\ldots$. This sequence of digits determines which subinterval $B_n(x) := I_{\varepsilon_1\ldots\varepsilon_n}$ at stage n contains x. Therefore, we find the Hölder exponent of x to be

$$\begin{aligned} \alpha^{\mu/\pi}(x) &= \lim_{n\to\infty} \frac{\log \mu(B_n(x))}{\log \pi(B_n(x))} \\ &= \lim_{n\to\infty} \frac{\log m_{\varepsilon_1} \cdot \ldots \cdot m_{\varepsilon_n}}{\log p_{\varepsilon_1} \cdot \ldots \cdot p_{\varepsilon_n}} \\ &= \lim_{n\to\infty} \frac{(1/n)\sum_{k=1}^{n} \log m_{\varepsilon_k}}{(1/n)\sum_{k=1}^{n} \log p_{\varepsilon_k}}. \end{aligned}$$

If we pick x uniformly, i.e. ε_k equals 0 and 1 with equal probability, then, we find by the LLN $\alpha^{\mu/\pi}(x) = \log(m_0 m_1)/\log(p_0 p_1)$ almost surely. To obtain results of the kind of large deviations, one has to change the probability of picking x such that the limit

$$\alpha^{\mu/\pi}(x)$$

takes other values than the 'expected' one.

In analogy with Subsection 2.1, pick $\varepsilon_k = i$ with probability $m_i^q p_i^{-\beta}$ where q is a free parameter and where

$$m_0^q p_0^{-\beta} + m_1^q p_1^{-\beta} = 1. \tag{7}$$

Denote the corresponding distribution of x by ϕ_q. Applying the LLN simultaneously to the random variables m_i and p_i yields that for ϕ_q-almost every x

$$\begin{aligned} \alpha^{\mu/\pi}(x) &= \frac{\mathbb{E}_{\phi_q}[\log m_i]}{\mathbb{E}_{\phi_q}[\log p_i]} \\ &= \frac{m_0^q p_0^{-\beta} \log m_0 + m_1^q p_1^{-\beta} \log m_1}{m_0^q p_0^{-\beta} \log p_0 + m_1^q p_1^{-\beta} \log p_1} \\ &= \beta'(q). \end{aligned} \tag{8}$$

This establishes the large deviation result and, consequently, a whole range of possible α-values. In addition, having explicitly constructed ϕ_q allows a rigorous computation of the Hausdorff dimension of $K_\alpha^{\mu/\pi}$, the set of μ/π-Hölder exponent α:

$$K_\alpha^{\mu/\pi} := \{x \in \mathbb{R}^d : \lim_{B\to\{x\}} \frac{\log \mu(B)}{\log \pi(B)} = \alpha\}.$$

We will not do so here, but rather furnish a simpler but less rigorous argumentation. It starts with the observation that $\alpha^{\mu/\pi}(x)$ is formally equal to the Hölder exponents observed for a more general construction of a 'binomial measure' ν: We start again with $J := [0,1]$ and choose two subintervals J_0 and J_1 with lengths in the proportion $p_0 : p_1$. At stage two, the four subintervals J_{00}, J_{01}, J_{10}, and J_{11} of this construction have, thus, lengths p_0p_0, p_0p_1, p_1p_0, and p_1p_1 respectively and ν-masses m_0m_0, m_0m_1, m_1m_0, and m_1m_1 respectively. At step n there are 2^n intervals $J_{\varepsilon_1\ldots\varepsilon_n}$ of length $|J_{\varepsilon_1\ldots\varepsilon_n}| = p_{\varepsilon_1} \cdot \ldots \cdot p_{\varepsilon_n}$ and mass $\nu(J_{\varepsilon_1\ldots\varepsilon_n}) = m_{\varepsilon_1} \cdot \ldots \cdot m_{\varepsilon_n}$.

The classical spectra $f_{\rm h}$ and $f_{\rm G}$ of ν are then well known [5, 1, 33]: $f_{\rm h} = f_{\rm G} = \beta^*$ where β is defined through (7). This allows to study $\alpha^{\mu/\pi}$.

First, let us comment on the coarse graining approach. Consider the intervals $J_{\varepsilon_1\ldots\varepsilon_m}$ of length $|J_{\varepsilon_1\ldots\varepsilon_m}| \simeq \delta$, more precisely, with m such that $p_{\varepsilon_1} \cdot \ldots \cdot p_{\varepsilon_m} < \delta \le p_{\varepsilon_1} \cdot \ldots \cdot p_{\varepsilon_{m-1}}$. Denote by $N_\delta(\alpha)$ the number of such intervals with 'coarse Hölder exponent' $\log \nu(J)/\log|J|$ approximately equal to α, i.e.

$$\frac{m_{\varepsilon_1} \cdot \ldots \cdot m_{\varepsilon_n}}{p_{\varepsilon_1} \cdot \ldots \cdot p_{\varepsilon_n}} \simeq \alpha. \tag{9}$$

Then [33],

$$N_\delta(\alpha) \simeq \delta^{-\beta^*(\alpha)}. \tag{10}$$

Here, $a(t) \simeq b(t)$ means $0 < c_1 < a(t)/b(t) < c_2 < \infty$ for some constants c_1, c_2. It is important to note that equation (10) can be viewed as a property of words $\varepsilon_1 \ldots \varepsilon_n$. More explicitly: $N_\delta(\alpha)$ is simply the number of words $\varepsilon_1 \ldots \varepsilon_n$ such that (9) and $p_{\varepsilon_1} \cdot \ldots \cdot p_{\varepsilon_n} \simeq \delta$ hold simultaneously.

In the contex of our multifractal analysis of μ with respect to π, words $\varepsilon_1 \ldots \varepsilon_n$ encode dyadic intervals $I_{\varepsilon_1\ldots\varepsilon_n}$ with length $|I| = 1/2^n$, $\mu(I) = m_{\varepsilon_1} \cdot \ldots \cdot m_{\varepsilon_n}$, and $\pi(I) = p_{\varepsilon_1} \cdot \ldots \cdot p_{\varepsilon_n}$. Hence, (10) describes the asymptotic behavior of the number of intervals $I_{\varepsilon_1\ldots\varepsilon_n}$ with $\pi(I) \simeq \delta$ and $\log \mu(I)/\log \pi(I) \simeq \alpha$. This translates to

$$f_R(\alpha) = \beta^*(\alpha).$$

Secondly, if one wants to conclude on the Hausdorff dimension of the set $K_\alpha^{\mu/\pi}$ some caution is required concerning the 'size' of sets. The most efficient covers of $K_\alpha^{\mu/\pi}$ are clearly provided by the

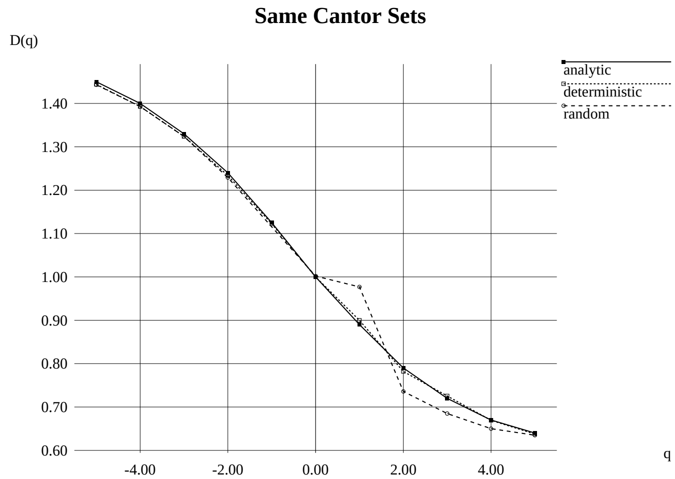

Figure 1: The relative multifractal dimensions D_R calculated via random and deterministic algorithms, and by solving (7) (solid line) in the case of two binomials (see Subsection 3.3). The parameters we used are $m_0 = .3$ $m_1 = .7$ and $p_0 = .5$, $p_1 = 0.5$. In order to add a slight complication we generalized the geometrical construction in choosing subintervals of relative length $l_0 = 0.25$ and $l_1 = 0.4$ for both, μ and π. While this procedure certinaly influences the usual spectrum $D(q)$, it will not affect D_R, and (7) still holds. As the measures have identical support, D_C will not provide any information other than $D(q)$. The order of approximation we used was $n = 13$, i.e. 2^{13} data points.

dyadic intervals $I_{\varepsilon_1 \ldots \varepsilon_n}$ with (9). Having a scaling law (10) in terms of $\pi(I) \simeq \delta$ instead of the usual $|I| \simeq \delta$ is again a simple consequence of the fact that we replace diameters of sets by $\pi(\cdot)$. So, (10) provides information not on the usual (Hausdorff) dimension but on the more general π-(Hausdorff) dimension. In simple terms, the π-dimension $\dim_\pi E$ of a set E is the critical exponent γ for which $\sum \pi(I_j)^\gamma$ remains bounded away from zero and infinity as $\{I_j\}_j$ forms an 'efficient' cover of E of smaller and smaller diameter. (See Billingsley [3] for an introduction to general dimensions. For $\pi(I) = |I|$ the usual Hausdorff dimension is recovered.) Covering the set $K_\alpha^{\mu/\pi}$ with dyadic intervals $I_{\varepsilon_1 \ldots \varepsilon_n}$ with (9) and $\pi(I_{\varepsilon_1 \ldots \varepsilon_n}) \simeq \delta$ we find $\sum \pi(I_{\varepsilon_1 \ldots \varepsilon_n})^\gamma \simeq N_\delta(\alpha)\delta^\gamma$ and conclude with (10) that

$$\dim_\pi K_\alpha^{\mu/\pi} = \beta^*(\alpha).$$

This formula has been found independently by Lvy Vhel and Vojak [22]. Note that its implicit formula $\alpha(q) = \beta'(q)$, $\beta^*(\alpha(q)) = q\alpha(q) - \beta(q)$ finds an explicit form by setting $c_i = \log p_i - \alpha \log m_i$:

$$\beta^*(\alpha) = \frac{c_2 \log(-c_2) + (c_1 - c_2)\log(c_1 - c_2) - c_1 \log(c_1)}{\log \lambda_1 \log p_2 - \log \lambda_2 \log p_1} \qquad (11)$$

for $\alpha \in]\alpha(\infty), \alpha(-\infty)[$, where we assumed without loss of generality that $\alpha(\infty) = \log p_1 / \log m_1 < \log p_2 / \log m_2 = \alpha(-\infty)$.

In order to compute the *usual* (Hausdorff) dimension one uses that for 'most' intervals $I_{\varepsilon_1 \ldots \varepsilon_n}$ with (9) we have

$$\begin{aligned} \frac{\log \pi(I_{\varepsilon_1 \ldots \varepsilon_n})}{\log |I_{\varepsilon_1 \ldots \varepsilon_n}|} &= \frac{-1}{n} \log_2 \pi(I_{\varepsilon_1 \ldots \varepsilon_n}) \simeq \\ \alpha^\pi(q) &= -m_0^q p_0^{-\beta} \log_2 p_0 - m_1^q p_1^{-\beta} \log_2 p_1. \end{aligned}$$

This follows actually from (8) and the fact that $K_\alpha^{\mu/\pi}$ concentrates the mass of ϕ_q. Then, $\sum |I_j|^\gamma \simeq N_\delta(\alpha)|I_{\varepsilon_1 \ldots \varepsilon_n}|^\gamma \simeq N_\delta(\alpha)\pi(I_{\varepsilon_1 \ldots \varepsilon_n})^{\gamma/\alpha^\pi(q)} \simeq \pi(I_{\varepsilon_1 \ldots \varepsilon_n})^{(\gamma/\alpha^\pi) - \beta^*(\alpha)}$ which is bounded exactly for $\gamma = \alpha^\pi(q) \cdot \beta^*(\alpha)$, the (usual) dimension of $K_\alpha^{\mu/\pi}$.

In summary, with $\alpha = \alpha(q) = \beta'(q)$,

$$\dim_\pi K_\alpha^{\mu/\pi} = \beta^*(\alpha) \qquad \dim(K_\alpha^{\mu/\pi}) = \beta^*(\alpha) \cdot \alpha^\pi(q).$$

Finally, the relative partition function is easely estimated:

$$S_\delta(q,t) = \sum_{C \in H_\delta} \mu(C^*)^q \pi(C^*)^{-t}$$

$$\simeq \sum (m_{\varepsilon_1} \cdot \ldots \cdot m_{\varepsilon_n})^q (p_{\varepsilon_1} \cdot \ldots \cdot p_{\varepsilon_n})^{-t}.$$

In the last sum the (finite) sequences $\varepsilon_1 \ldots \varepsilon_n$ encode the various $C \in H_\delta$. It is easy to verify that this sum equals exactly 1 when setting $t = \beta(q)$. Thus,

$$\tau_R(q) = \beta(q). \tag{12}$$

For a typical graph see Fig. 1 where $D_R(q) = \tau_R(q)/(q-1)$ is plotted (solid line). In summary:

Theorem 1 *In the simple case where μ and π are binomial measures the* multifractal formalism *holds:*

$$\dim_\pi K_\alpha^{\mu/\pi} = f_R(\alpha) = {\tau_R}^*(\alpha). \tag{13}$$

In addition, the implicit formulas (12) and (7) can be made explicit (11).

The fact that the multifractal formalism holds shows again that the π-dimension is more natural in this context than the usual Hausdorff dimension.

In addition, the **difference between conditional and relative spectrum** becomes clear. Still in the binomial case we have

$$f_{\rm C}(\alpha) = f_{\rm h}(\alpha) = f_{\rm G}(\alpha) = \tau^*(\alpha),$$

where τ^* is the Legendre transform of $\tau(q) = -\log_2({m_0}^q + {m_1}^q)$. Thus, the conditional spectrum of μ coincides here with the usual multifractal spectra and provides no information about the reference measure. In particular, the p_i are not involved.

To the contrary, with the relative spectrum $f_R(\alpha)$ which reveals to what extent the geometries of μ and π coincide: This spectrum reduces to a point if and only if the singularities of μ and π are identical, i.e. if $m_i = p_i$. The wider the graph of $f_R(\alpha)$ is, the more the two distributions differ. More precisely, if it is scewed to the left, i.e. if the minimal α is closer to 1 than the maximal one, then the two distributions match better in the dense parts than in the sparse parts, and vice versa.

One may argue that it is unnatural to consider distributions which are 'manifesting' in the same points as is the case with the binomial measures. Before commenting on the general case in Subsection 3.4 we would like to mention an example where exactly this situation is met: the traffic load on a network [40]. Here, the number of bytes in a packet and its arriving time are recorded. Letting μ be the amount of work arriving and π the time between arrivals we have a string of data which we may consider as being given in the dyadic points of some order n. It is natural, then, to be interested in the difference of the spectra when analyzing the workload with respect to arrival time (i.e. the number of packets having already arrived, which corresponds to $|\cdot|$) and with respect to real time (which corresponds to π).

Moreover, the purpose of this section was to show the main features of the new approach on a simple example without adding unneccessary complication. Without going into detail we mention the more general discontinuous self-similar measures which may consist of atoms located in the dyadic points, say μ, or in the triadic points, say π (for details see [25, 35, 36]). This is a more natural assumption. Since the dyadic and the triadic points are dense, the same conclusion as above holds: The conditional spectrum of μ with respect to π coincides with the usual spectrum while the relative spectrum provides information on the mutual dependence of the two distributions μ and π:

$$f_{\rm C}(\alpha) = f_{\rm G}(\alpha) \neq f_R(\alpha).$$

3.4 Presence of gaps

So far we have discussed the new notions for two measures μ and π which are supported on the same set, an assumption we are going to drop now.

Overlapping supports: As a first step consider two b-nomial measures μ and π. These measures are constructed similarly as the binomial measure in Subsection 2.1 with the only change that we distribute mass now among b subintervals of equal length instead of just among two. Thus, at first stage we have b intervals $[i/b, (i+1)/b]$ with μ mass m_i and π mass p_i $(i = 0, \ldots, b-1)$, etc.

In the first case we consider the reference measure π lives on a Cantor set with dimension strictly less than 1. This is equivalent to saying that some of the probabilities p_i are 0. Since the support of μ is the interval $[0,1]$, it contains the support of the reference measure π which is a Cantor set. For convenience we write $\mathrm{spt}(\mu) > \mathrm{spt}(\pi)$. In this case it is easy to verify that all results of Subsection 3.3 are still valid given the convention $0^q := 0$ in (7).

With the roles exchanged, i.e. μ living on a b-adic Cantor set and the reference measure π being supported on the whole interval ($\mathrm{spt}(\mu) < \mathrm{spt}(\pi)$), the same is still true for the spectrum of dimension of $K_\alpha^{\mu/\pi}$. The approach via partition function needs, however, special attention. We will address numerical implications in Section 4 which provides the appropriate context. Here, we mention a closely related 'integral version'.

Instead of coarse graining, i.e. subdividing space into boxes, multifractal analysis may also follow an approach relying on ideas of 'dynamical systems'. The generalized dimensions can then be directly observed from the longtime behaviour of orbits as described in [13, 19]: In order to approximate a distribution one follows a generic trajectory of the system. In our situation this is obtained by setting $x_{n+1} = x_n/b + i$ where i is picked with probability p_i. One takes a ball B_n of diameter δ around x_n and averages $\mu(B_n)^q \pi(B_n)^{-t-1}$ over some N sample points x_n:

$$S_\delta(q,t) = \sum_{n=1}^{N} \mu(B_n)^q \pi(B_n)^{-t-1} \sim \sum_{B} \mu(B)^q \pi(B)^{-t} \qquad (14)$$

This approach is naturally very closely related to the 'integral version' of $S_\delta(q,t)$ which is of importance in the theory of dynamical systems [29, 30, 33]:

$$S_\delta(q,t) = \int \mu(B_\delta(x))^q \cdot \pi(B_\delta(x))^{-t-1} d\pi(x).$$

This integral, unfortunately, does not converge for q below some negative threshold q_{bottom} in the case $\text{spt}(\mu) < \text{spt}(\pi)$ [34]. The integral

$$S_\delta(q,t) = \int \mu(B_\delta(x))^q \cdot \pi(B_\delta(x))^{-t-1} d\mu(x),$$

on the other hand, does converge under the same assumption $\text{spt}(\mu) < \text{spt}(\pi)$. Therefore, the two measures μ and π can not be used equivalently with the integral approach.

Distinct supports: As the supports of μ and π become more distinct, general results are not available at this time. The definition of $K_\alpha^{\mu/\pi}$ makes certainly no sense if the supports of μ and π have no points in common. If the supports of μ and π come close enough, however, coarse graining methods will still show most of the features described above since numerical analysis always has to stop before the actual limit $\delta \to 0$.

For a more rigorous argument consider two distributions where we assume that the sum of the dimensions of the supports of these measures is larger than 1. Then it is known that we find two points from the different distribution at arbitrary small distance. Consequently, for every δ we can find a cube C in the grid G_δ which contains at least one point from each distribution. Now, rewrite the Hölder exponent of C^* as

$$\alpha(C^*) = \frac{\log \mu(C^*)/\log \delta}{\log \pi(C^*)/\log \delta}$$

and use the fact that $\underline{\alpha} := D^\mu(\infty)$ is the smallest, resp. $\bar{\alpha} := D^\mu(-\infty)$ the largest Hölder exponent of μ. (This follows from the multifractal formalism, in particular Corollary 2, which we establish in the appendix). Thus, we find that $D^\mu(\infty)/D^\pi(-\infty) \le \alpha(C^*) \le D^\mu(-\infty)/D^\pi(\infty)$. In particular, $D_R(\infty) = \inf D_R(q) = \inf \alpha^{\mu/\pi}$ and $D_R(-\infty) = \sup D_R(q)$ are not degenerate. The deviation of $D_R(\infty)$, resp. $D_R(-\infty)$ from the theoretically smallest, resp. largest possible value $\underline{\alpha}$, resp. $\bar{\alpha}$ gives information on the correlation of sparse parts of μ and dense parts of π, and vice versa (compare Subsection 4.3).

It is in this context with a presence of gaps where the more straightforward conditional spectrum D_C becomes meaningful since it profits from the similar effects as the ones we just described for D_R. We refer in particular to Fig. 1 and 3, as well as to Section 4.

4 Numerical aspects

We are now describing the algorithms used and give an interpretation of the various spectra through some numerical simulations.

The numerical situation is simple as long as both measures μ and π are supported on the whole interval $[0,1]$. The presence of gaps causes, however, two kinds of numerical problems which call for different solutions for D_C and D_R. After elaborating on this essential issue in Subsection 4.1 and 4.2 we close by interpreting some numerical simulations.

4.1 Numerical stability

The presence of gaps causes two kinds of numerical problems. First, the cubes C chosen from a grid G_δ may be 'misplaced'. More precisely, C may be a very poor approximation of a ball centered in points of the distribution it contains. Consider for instance the analysis of a 3-nomial measure μ with respect to a 4-nomial reference measure π. Then, it is impossible to chose grid-sizes to match the geometry of both measures. (In any case, a numerical method which requires knowledge on the distribution μ *in advance* is worthless.)

Such 'misplaced' cubes result in unnaturally large contributions $\mu(C)^q$, resp. $\pi(C)^{-t}$ for negative q respectively positive t. This is the major cause of numerical instability in that regime. It has been shown

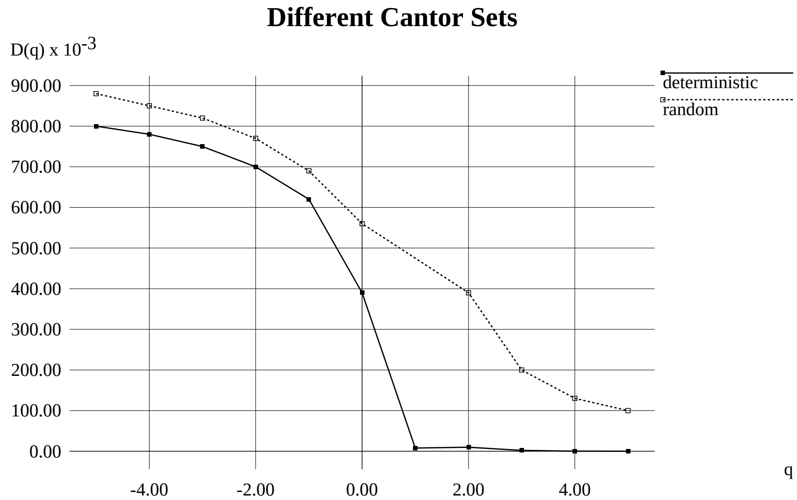

Figure 2: The relative multifractal dimensions D_R estimated by the deterministic and the random algorithms in the case of different supports for μ and π. The parameters are $l_0 = 0.25$, $l_1 = 0.4$, $m_0 = 0.6$, $m_1 = 0.4$, for the analyzed measure μ, and $\lambda_0 = 0.3$, $\lambda_1 = 0.33$, $p_0 = 0.7$, $p_1 = 0.3$ for the reference measure π.

[33, 28], that this problem can be removed by simply imploying the enlarged cubes C^* introduced earlier.

4.2 Partitioning: deterministic versus random algorithm

As a second problem caused by gaps we would like to address the partition into sets C of roughly equal mass $\pi(C) \simeq \delta$ instead of equal diameter. This method has advantages in particular when computing the *relative* multifractal dimensions $D_R(q)$: with the term $\pi(C^*)$ being roughly independent of C, the definition of $\tau_R(q)$ reduces to the usual $\sum_C \mu(C^*)^q \simeq \delta^{\tau_R}$. Thus, $\tau_R(q)$ can be obtained as the slope of a log-log plot of $\sum_C \mu(C^*)^q$ against δ.

For a computation of D_C, on the other hand, such a procedure is not necessary. The only information draw from the reference measure π is whether or not $\pi(C) = 0$. So, a usual partition G_δ into intervals of equal size δ is sufficient here.

Remark: Partitions H_δ with $\pi(C) \simeq \delta$ are also imployed with the so-called 'fixed mass algorithm' which is bound to compute the ordinary f_{G} spectrum for π itself. In our approach, on the other hand, H_δ is used in order to provide a fast algorithm for computing D_R.

Difficulties arise when trying to find such a partition with $\pi(C) \simeq \delta$.

Working on the line one might order the points $\{x_n\}_{n=0}^N$ which constitute the reference distribution and consider partitions $[x_{nk}, x_{(n+1)k}[$ $(n = 0, \ldots, (N-1)/k)$ with $\delta = k/N$ $(k > 2)$. We call this method the **deterministic algorithm**. While it works certainly well when π has full support or when μ and π have identical support, it can lead to wrong results in the presence of gaps.

For numerical evidence we put forward Fig. 1 and2. For a theoretical argumentation consider a 3-nomial measure with $p_0 \neq 0 = p_1 \neq p_2$ as the reference measure π. Then, certain triadic intervals, such as $[1/3, 2/3]$, will contain no 'reference point' x_n. Unless we are very lucky, for every k one of the intervals $[x_{nk}, x_{(n+1)k}[$ will contain the whole interval $[1/3, 2/3]$, one will contain $[1/9, 2/9]$, one $[7/9, 8/9]$ etc. Since it is very unlikely that the points x_{nk} fall exactly on the critical points $1/3$, $2/3$, $1/9$ etc. The intervals obtained by such a 'deterministic' partition are, again, very poor approximations of balls centered in points of the distribution π. To make this statement more rigorous we offer the following reasoning. The distribution μ, in contrary to π, will in general have a considerable amount of mass inside these gaps. For a 4-nomial measure μ with $m_2 = 0$, i.e. mass m_0 in $[0, 1/4]$, m_1 in $[1/4, 2/4]$, no mass in $[2/4, 3/4]$ and mass m_3 in $[3/4, 1]$, the whole interval $[7/16, 8/16]$ with mass $m_1 \cdot m_3$ will be contained in

$[1/3, 2/3]$. This means that intervals with fewer and fewer reference points contain a μ-mass which does not tend to zero but remains larger than $m_1 \cdot m_2$. As a consequence, $\sum_C \mu(C^*)^q$ is basically constant in δ for large q, which is a considerable loss of information. This is most strikingly demonstrated with Fig. 2.

Another method of constructing a partition with $\pi(C) \simeq \delta$ was introduced with $\boldsymbol{H_\delta}$ in Subsection 3.2. With this approach, we find difficulties when the reference measure is atomic.

Finally, the **random approach** which we introduced with (14) was found to be most fruitful and reliable in the presence of gaps and with distinct supports (see Fig. 2).

4.3 Numerical simulations

According to Subsection 4.2 we estimated D_C using the classical 'equal length' partition G_δ. This means in practice that we divide the line into intervals of length δ and take into account the mass only of such intervals which contain at least one point from the reference distribution too. For the estimation of D_R, on the other hand, we applied the random method. While the three spectra produce about the same values for negative q, the differences become meaningful for positive q (dense parts of the distribution).

As Fig. 1 demonstrates, the numerical result of $D_R(q)$ gives a slight overestimation of the exact result. If q is nearby one, however, the simulated results are essentially different from the expected theoretical value. This is a consequence of the normalization [28], which becomes necessary due to our use of C^*. For large $|q|$, on the other hand, we have very good results, which is notable in particular for $q < 0$.

In Fig. 1 the measures μ and π have identical support. Here, the deterministic algorithm is slightly more accurate. Fig. 2, on the other hand, demonstrates very well, how a deterministic method of chosing a partition can be very misleading in a general situation.

Before proceeding to a comparison between D_C and D_R let us recall some fundamental features of these novel multifractal notions. The following statements follow from the discussion in Subsection 3.3, in particular from (7), as well as from the multifractal formalism Corollary 2 (see the appendix).

- If D_C equals the usual multifractal dimensions $D(q)$, not much can be said: The support of μ is contained in the support of the reference measure π.
- The more D_C differs from $D(q)$ the more depends its geometry on the mere presence of reference points.
- If D_R equals $D(q)$ then the reference measure is equivalent to 'volume' on the support of μ.
- As with D_C, a deviation of D_R from $D(q)$ for $q \to \pm\infty$ gives information on how much the reference measure differs from uniform distribution (or 'volume') in the dense, resp. sparse parts of μ.
- If D_R is a constant — the value of which is necessarily 1 — then the analyzed measure and the reference measure can be considered to be equivalent from multifractal point of view.
- The wider the range of D_R the more complex the mutual dependence of the geometries of the two distributions. A small $D_R(\infty)$ implies the existence of dense μ-parts with only sparse reference points and vice versa if $D_R(-\infty)$ is large.

In summary, both, D_C and D_R are most conveniently compared with $D(q)$ for $q \to \pm\infty$. In addition, D_R has an interpretation in absolute terms, i.e. in its deviation from a constant (compare Subsection 3.4).

Let us now interpret the conditional spectrum and the relative spectrum for the instructing example in Fig. 3.

Looking first at D_C, which is simpler to interpret, we conclude that the mutual dependence is much stronger in the dense parts of μ than in its sparse parts.

From the shape of D_R we deduce that the distributions μ and π are rather different from multifractal points of view. In addition, in the sparse parts of μ we find that π behaves like the uniform distribution, while there are places where the μ-points fall rather dense and where reference points fall less dense than compared with uniform distribution or 'volume'. This we deduced from $D_R(-\infty) \simeq D(-\infty)$ and from $D_R(\infty)$ being essentially smaller than $D(\infty)$.

Although not displayed in the figure it is generally true that the standard errors of estimated relative dimensions D_R are roughly half as big as the ones of conditional dimensions D_C for negative q.

In summary

- The deterministic method works well when π has full support or when μ and π have identical support.

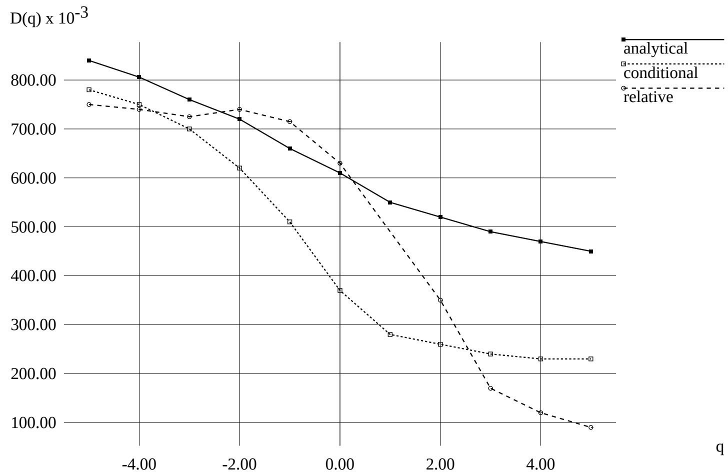

Figure 3: A comparison of the relative multifractal dimensions D_R (estimated with random algorithm) and the conditional multifractal dimensions D_C (estimated with deterministic algorithm) in a situation similar to Fig. 2. The parameter values are as in Fig. 2 with the sole exception that the geometrical parameters λ_0 and λ_1 of π have been interchanged. The solid line refers to the classical multifractal dimensions $D(q)$ of μ, estimated numerically from the same data as D_R and D_C, rather than solving the transcendent equation $m_0^q l_0^{-\tau} + m_1^q l_1^{-\tau} = 1$. Comparing the dimensions for $q \to -\infty$ (sparse parts of the distribution) and $q \to \infty$ we may conclude that the mutual dependence is much stronger in the dense parts.

- The random algorithm has to be applied in the presence of gaps.
- While D_C provides a fast algorithm and is more easy to interpret, D_R is in general more informative.
- As a general rule the standard errors for D_C are twice as large as the ones for D_R, at least for negative q.
- Useful information is obtained from comparing the various spectra, in particular the extremal values at $q = \pm\infty$.

Conclusions.

We introduced two novel multifractal notions $D_C(q)$ and $D_R(q)$ which are helpful in describing the relation and dependence of the fractal geometry of two distributions of points on each other. As was pointed out, special information can be gained from $q = 0$ and $q \to \pm\infty$ as well as from comparing $D_C(q)$ and $D_R(q)$ with the usual generalized dimensions $D(q)$.

Acknowledgement.

We would like to thank T. Vicsek for pointing out the reference [2]. RHR gratefully acknowledges financial support, which he received in part by the Office of Naval Research (ONR grant N00014-90.J.1026) and in part by the Swiss National Foundation of Science. During the time of this research, IS was supported by OTKA T 019524.

References

[1] M. Arbeiter and N. Patzschke, Self-Similar Random Multifractals, *Math. Nachr.* **181** (1996) pp 5–42

[2] C. Beck, Upper and lower bounds on the Renyi dimensions and the uniformity of multifractals *Physica D* **41** (1990) pp 67–78

[3] Billingsley, *Ergodic Theory and Information*, Chapter 14 Wiley New York (1965),

[4] G. Brown, G. Michon and J. Peyriere On the Multifractal Analysis of Measures *J. Stat. Phys.*: **66** (1992) pp 775–790

[5] R. Cawley and R. D. Mauldin, Multifractal Decompositions of Moran Fractals, *Adv. in Math.* **92** (1992) pp 196–236

[6] V. R. Chechetkin, Multifractal structure of fully developed hydrodynamic turbulence II, *Stat. Phys.* **61** (1990) pp 589

[7] S. Chen and H. Zhao, Fat fractal and multifractals for protein and enzyme surfaces, *Intern. J. Bio. Macromolecules* **13** (1991) pp 210

[8] P. Collet, J. Lebovitc and A. Porcio, The Dimension Spectrum of Some Dynamical Systems, *J. Stat. Phys.* **47** (1987) pp 609–644.

[9] A. Czirók, P. Szépfalusy and T. Vicsek, On the existence of well defined singularities in multifractals *Fractals.* **1** (1993) pp 199–204.

[10] Richard Ellis Large Deviations for a general Class of Random Vectors *Ann. Prob.* **12** (1984) pp 1–12.

[11] K. J. Falconer, Fractal Geometry: Mathematical Foundations and Applications, John Wiley and Sons, New York (1990)

[12] Frisch and Parisi, Fully developed turbulence and intermittency *Proc. Int. Summer school on 'Turbulence and Predictability in Geophysical Fluid Dynamics and Climate Dynamics'* (North-Holland 1985) pp 84–88

[13] P. Grassberger, Generalized Dimensions of strange attractors, *Phys. Lett. A* **97** (1983) pp 227–230.

[14] Peter Grassberger, Generalizations of the Hausdorff Dimension of Fractal Measures, *Phys. Lett. A* **107** (1985) pp 101–105.

[15] P. Grassberger and I. Procaccia, Characterization of strange attractors, *Phys. Rev. Lett.* **50** (1983) pp 346–349.

[16] P. Grassberger and I. Procaccia, Measuring the strangeness of strange attractors, *Physica D* **9** (1983) pp 189–208.

[17] T. Halsey, M. Jensen, L. Kadanoff, I. Procaccia and B. Shraiman Fractal measures and their singularities: The characterization of strange sets *Phys. Rev. A* **33** (1986) pp 1141–1151

[18] H. M Hastings and G. Sugihara *Fractals, a user's guide for the natural sciences* Oxford Univ. Press. Oxford (1993) ISBN 0-19-854598-3

[19] H. Hentschel and I. Procaccia The Infinite number of Generalized Dimensions of Fractals and Strange Attractors *Physica D* **8** (1983) pp 435–444

[20] M. Jensen, L. Kadanoff and I. Procaccia Scaling structure and thermodynamics of strange sets *Phys. Rev. A* **36** (1987) pp 1409–1420.

[21] K.-S. Lau and S.-M. Ngai, Multifractal Measures and a Weak Separation Condition, *Adv. Math.* accepted for publication (1995).

[22] J. Levy-Vehel and R. Vojak, Multifractal analysis of Choquet capacities: Preliminary Results, *Adv. Appl. Math.* to appear (1997).

[23] B. B. Mandelbrot, *The Fractal Geometry of Nature*, New York Freeman (1982).

[24] B. B. Mandelbrot, Intermittent turbulence in self similar cascades : divergence of high moments and dimension of the carrier *J. Fluid. Mech.* **62** (1974) p 331

[25] B. B Mandelbrot and R. H. Riedi, Inverse Measures, the Inversion formula and Discontinuous Multifractals, *Adv. Appl. Math.* **18** (1997) pp 50–58.

[26] B. T Milne, Spatial aggregation and neutral models in fractal landscapes, *American Naturalist* **139** (1992) pp 32–57

[27] E. Ott, W. Withers and J. Yorke, Is the Dimension of Chaotic Attractors invariant under Coordinate Changes? *J. Stat. Phys.* **36** (1984) pp 687–697.

[28] R. Pastor-Satorras and R. Riedi, Numerical Estimates of Generalized Dimensions D_q for Negative q, *J. Phys. A: Math. Gen.* **29** (1996) L391–L398

[29] Ya. B. Pesin, On the Notion of the Dimension with Respect to a Dynamical System, *Ergod. Th. Dynam. Sys.* **4** (1984) pp 405–420

[30] Ya. B. Pesin, On Rigorous Mathematical Definitions of Correlation Dimension and Generalized Spectrum for Dimensions, *J. Stat. Phys.* (1995)

[31] Ya. B. Pesin, Generalized Spectrum for the Dimension: the Approach Based on Caratheodory's Construction, in *Constantin Caratheodory, an International Tribute*, ed. by ThM. Rassias, **2** (1991) pp 1108–1119

[32] B. Rajagopalan and D. G. Tarboton, Understanding complexity in the structure of rainfall, *Fractals* **1. 3** (1993) pp 606–616

[33] R. H. Riedi, An Improved Multifractal Formalism and Self-Similar Measures, *J. Math. Anal. Appl.* **189** (1995) pp 462–490

[34] R. H. Riedi, Seven approaches to Multifractal Analysis: an introduction *forthcoming*

[35] R. H. Riedi and B. B Mandelbrot, Inversion formula for Continuous Multifractals, *Adv. Appl. Math.* **19** (1997) pp 332–354

[36] R. H. Riedi and B. B Mandelbrot, Exceptions to the Multifractal Formalism for Discontinuous Measures, *Math. Proc. Cambr. Phil. Soc.* **123** (1998) pp 133–157.

[37] I. Scheuring and R. Riedi Application of multifractals to the analysis of vegetation pattern *J. Veg. S.* **5** (1994) pp 489–496

[38] R. Strichartz, Self-Similar Measures and their Fourier Transforms III, *Indiana Univ. Math. J.* **42** (1993) pp 367–411

[39] Tamás Vicsek *Fractal Growth Phenomena* World Scientific, Singapore, 1989

[40] added in proof: R. Riedi and J. Lévy Véhel, Multifractal Properties of TCP Traffic: a Numerical Study. submitted *ACM SIGCOMM* (1997) http://www-syntim.inria.fr/fractales/

Appendix

Coarse graining methods for general reference measures

For the coarse grained version of the relative multifractal spectrum in full generality one uses similar ideas as for the partition function $\tau_R(q)$ defined in Subsection 3.2. One has to replace the simple 'counting' of the boxes C with $\mu(C^*) \sim |C^*|^\alpha$ by

$$N_{\delta,\varepsilon}(\alpha,\gamma) := \sum_{\delta,\varepsilon}^{\alpha} \pi(C^*)^\gamma$$

where the sum $\sum_{\delta,\varepsilon}^{\alpha}$ runs over all $C \in G_\delta$ with $\pi(C^*)^{\alpha+\varepsilon} \le \mu(C^*) < \pi(C^*)^{\alpha-\varepsilon}$. In other words, one does not count the *boxes* C with the desired property but the *sample points* of the reference measure π which can be found in such boxes C.

Then, one defines the *relative coarse grained spectrum* as

$$f_R(\alpha) := \lim_{\varepsilon\to 0} \inf\{\gamma \,:\, N_{\delta,\varepsilon}(\alpha,\gamma) \to 0 \text{ as } \delta \to 0\}$$

which generalizes the usual notion as given in Subsection 3.2. We have:

Lemma 2

$$\tau_R(q) = \inf_{\alpha\in\mathbb{R}} \big(q\alpha - f_R(\alpha)\big).$$

Proof
Fix q. Note first that we may estimate

$$\begin{aligned} S_\delta(q,t) &\ge \sum_{\delta,\varepsilon}^{\alpha} \mu(C^*)^q \pi(C^*)^{-t} \\ &\ge \sum_{\delta,\varepsilon}^{\alpha} \pi(C^*)^{q\alpha+|q\varepsilon|-t} \\ &= N_{\delta,\varepsilon}(\alpha, q\alpha+|q\varepsilon|-t). \end{aligned}$$

Now, assume that $t > q\alpha - f_R(\alpha)$ for some α. Choose ε small enough so that $q\alpha + |q\varepsilon| - t < f_R(\alpha)$. Then, by making ε even smaller if neccessary, there is a sequence $\delta_n \to 0$ and $c > 0$ such that $N_{\delta_n,\varepsilon}(\alpha, q(\alpha \pm \varepsilon) - t) \ge c$. This yields

$$S_{\delta_n}(q,t) \ge c$$

hence, $\tau_R(q) \le t$. We conclude that $\tau_R(q) \le q\alpha - f_R(\alpha)$. Since α was arbitrary, $\tau_R(q) \le \inf q\alpha - f_R(\alpha)$. The opposite estimate is obtained with similar methods, but writing more carefully

$$S_\delta(q,t) = \sum_k \sum_{\delta,\varepsilon}^{\alpha_k} \mu(C^*)^q \pi(C^*)^{-t}$$

with $\alpha_k = k\varepsilon$. For details see [11, 33, 34]. $\diamondsuit$

Since $\tau_R(q)$ is concave we find :

Corollary 1 *The* relative multifractal dimensions

$$D_R(q) := \frac{\tau_R(q)}{q-1}$$

are monotone as a function of q.

Corollary 2 (Multifractal formalism) *The relative multifractal spectrum* $f_R(\alpha)$ *can be obtained from* $\tau_R(q)$ *as in (6). Moreover,* $D_R(\infty)$ *and* $D_R(-\infty)$ *are the minimal and the maximal relative Hölder exponent* $\alpha^{\mu/\pi}$.